MolecularMedicine

Supplemental Data

Aspirin's Active Metabolite Salicylic Acid Targets High Mobility Group Box 1 to Modulate Inflammatory Responses

Hyong Woo Choi,[1] Miaoying Tian,[1†] Fei Song,[2*] Emilie Venereau,[4] Alessandro Preti,[4] Sang-Wook Park,[1‡] Keith Hamilton,[2] G V T Swapna,[2] Murli Manohar,[1] Magali Moreau,[1] Alessandra Agresti,[4] Andrea Gorzanelli,[4] Francesco De Marchis,[4] Huang Wang,[2] Marc Antonyak,[5] Robert J Micikas,[1] Daniel R Gentile,[1§] Richard A Cerione,[5] Frank C Schroeder,[1] Gaetano T Montelione,[2,3] Marco E Bianchi,[4] and Daniel F Klessig[1]*

Online address: http://www.molmed.org

The Feinstein Institute for Medical Research
North Shore LIJ
Empowering Imagination. Pioneering Discovery.®

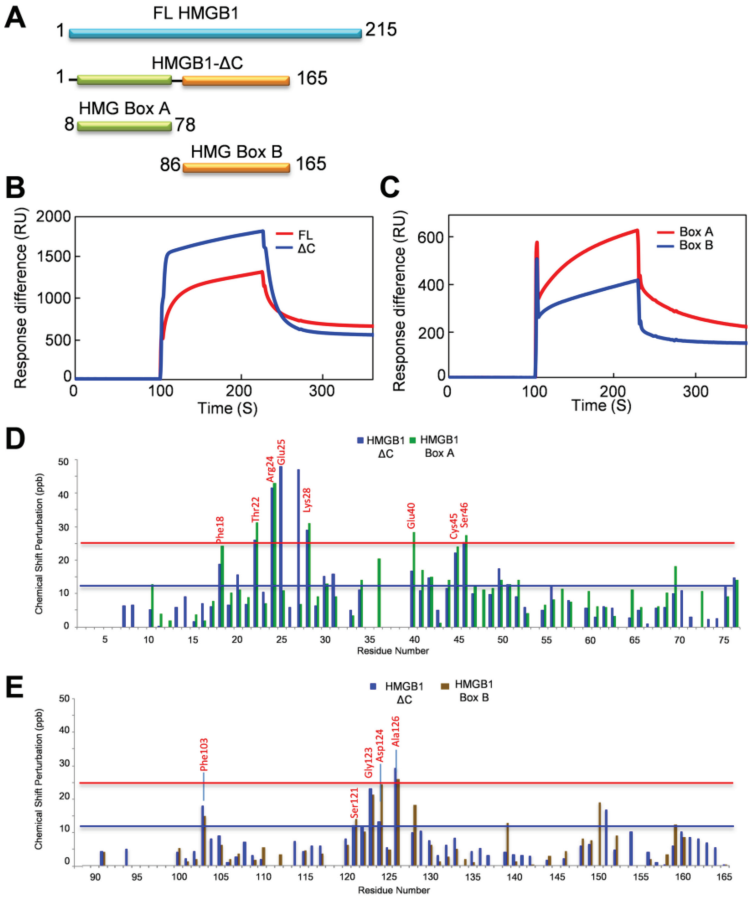

Supplementary Figure S1. Evaluation of the SA-binding activity of various HMGB1 constructs by SPR and NMR. (A) Schematic showing the residue boundaries of constructs of full-length (FL) HMGB1, HMGB1-ΔC, Box A and Box B used for SPR and NMR studies. (B) Sensorgrams of recombinant FL HMGB1 (4 μM) and HMGB1-ΔC (4 μM) interacting with 3AESA immobilized on the sensor chip. (C) Sensorgrams of recombinant Box A and Box B (4 μM) interacting with 3AESA immobilized on the sensor chip. The signal from the mock-coupled surface was subtracted. Note the binding kinetics of Box A and Box B cannot be compared directly since the analysis of each was done on different sensor chips and on different days. (D and E) CSPs plotted as a function of residue number for three HMGB1 constructs. CSPs for Box A are shown in green in (D) and those for Box B in brown in (E). CSPs for the HMGB1-ΔC construct, in blue, are also plotted in both (D) and (E). Thresholds used for mapping CSPs onto the 3D structures are shown at 12 ppb (blue horizontal line) and 25 ppb (red horizontal line).

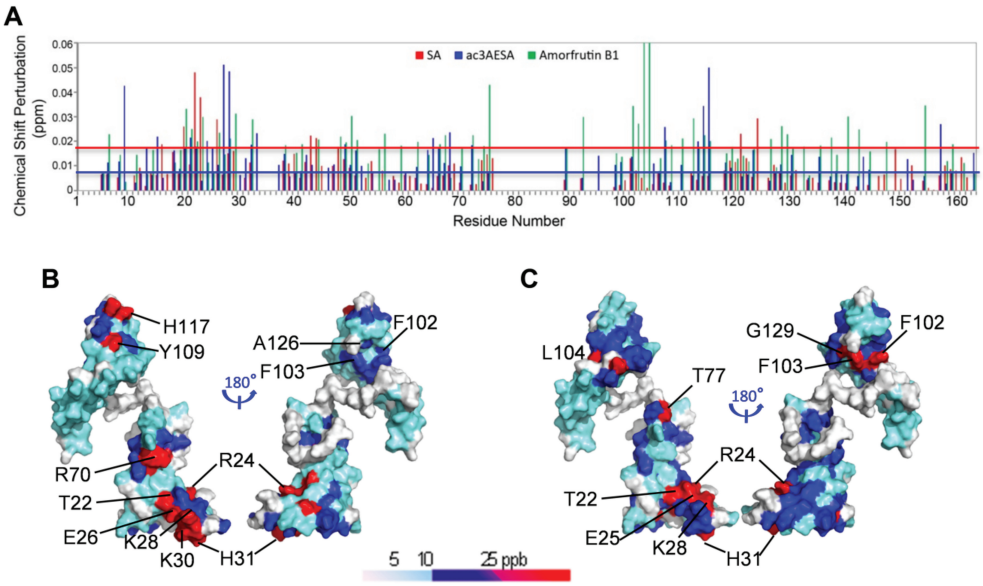

Supplementary Figure S2. SA, ac3AESA, and amorfrutin B1 share the same binding sites in HMGB1. (A) Chemical shift perturbations of FL HMGB1 arising from 15 mM SA (red), 3 mM ac3AESA (blue) and 2 mM amorfrutin B1(green). Thresholds used for mapping CSPs onto the 3D structures are shown at 12 ppb (blue horizontal line) and 25 ppb (red horizontal line). (B and C) Ac3AESA (B) and amorfrutin B1 (C) induced CSPs mapped onto the 3D structure of human HMGB1-ΔC (2YRQ, residues 6-164). The colors correspond to the amplitude of the observed $\Delta\delta_{(N-H)}$ CSPs (cyan: $\Delta\delta_{(N-H)}$ < 12 ppb; blue: 12 < $\Delta\delta_{(N-H)}$ < 25 ppb; red: $\Delta\delta_{(N-H)}$ > 25 ppb, as indicated by the scale). Residues for which the backbone ^{15}N-^{1}H resonance assignments are not available due to rapid exchange of surface amide protons and/or proline residues, are shown in white.

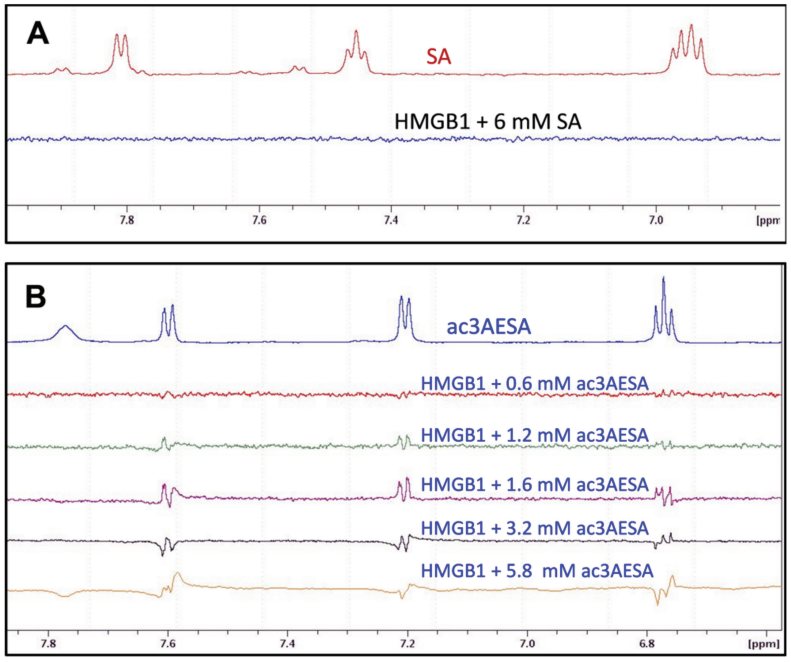

Supplementary Figure S3. Saturation transfer difference (STD) results demonstrating that ac3AESA has stronger binding affinity to HMGB1 than SA. Ligand-detected STD experiments using 6 mM SA (A) or a titration using 0.6 to 5.8 mM ac3AESA (B), with 20 μM FL HMGB1. In each panel, the top trace is the spectrum of the ligand (SA in the top panel and ac3AESA in panel B), and the traces below these are the STD spectra with various amounts of ligand added. These results demonstrate a STD effect for HMGB1 binding by ac3AESA at concentrations greater than about 1 mM, but no STD effect for HMGB1 binding by SA at concentrations as high as 6 mM under the conditions of these measurements (final buffer conditions 140 mM NaCl, 3 mM KCl, 10 mM $Na_2H(PO_4)$, 1.8 M $KH_2(PO_4)$, pH 7.4).

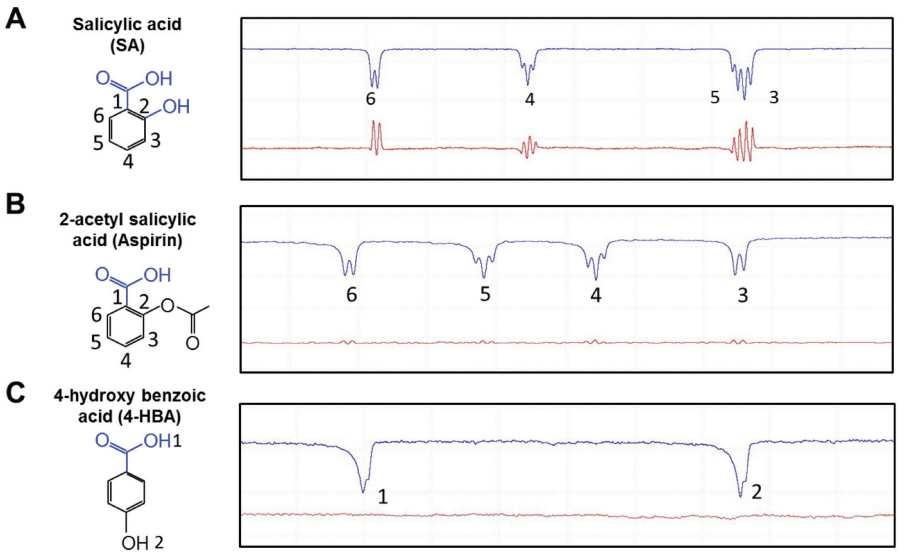

Supplementary Figure S4. HMGB1 binds SA, but neither aspirin nor 4-hydroxy benzoic acid (4-HBA). (A-C) Ligand-detected WaterLogsy experiments using 20 μM HMGB1 with 6 mM SA (A), 6 mM aspirin (B) or 6 mM 4-HBA (C). The top blue trace in (A-C) shows the 1D spectrum of SA (A), aspirin (B), or 4-HBA (C). The numbered peaks correspond to the resonances assignments to protons in the left panels. The lower red trace in (A-C) shows the WaterLogsy spectrum of HMGB1 with SA (A), aspirin (B), or 4-HBA (C). 1D spectra of the aspirin sample used for NMR analyses indicated that it was free of SA that can result from breakdown of aspirin.

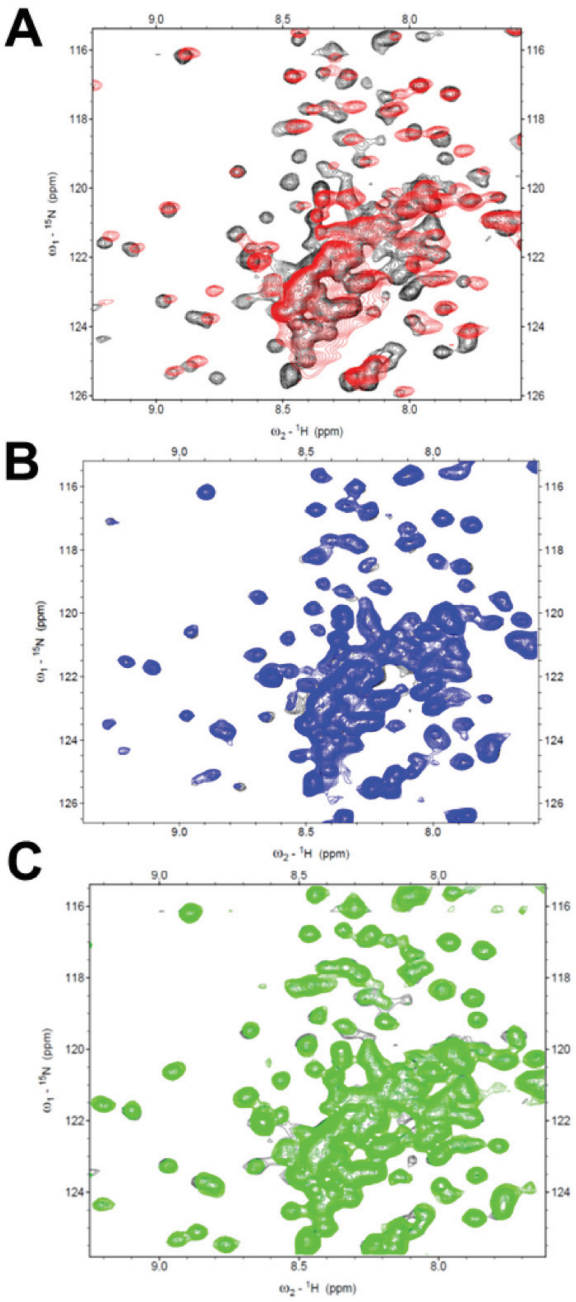

Supplementary Figure S5. Superimposed ^{15}N-^{1}H TROSY-HSQC spectra of FL HMGB1 (residues 1-214; ~0.2 mM protein concentration) recorded in the absence (black) or presence of 10 mM SA (red) in (A), absence (black) or presence of 10 mM aspirin (blue) in (B), and absence (black) or presence of 10 mM 4-hydroxy benzoic acid (4-HBA; green) in (C). All spectra were acquired at 20°C on a Bruker 800 MHz NMR spectrometer equipped with a 4 mm cryoprobe. 2048 complex points were acquired for each of the 128 increments in the ^{15}N dimension with a recycle delay of 1 s. Each spectrum was acquired for 1.5 h.

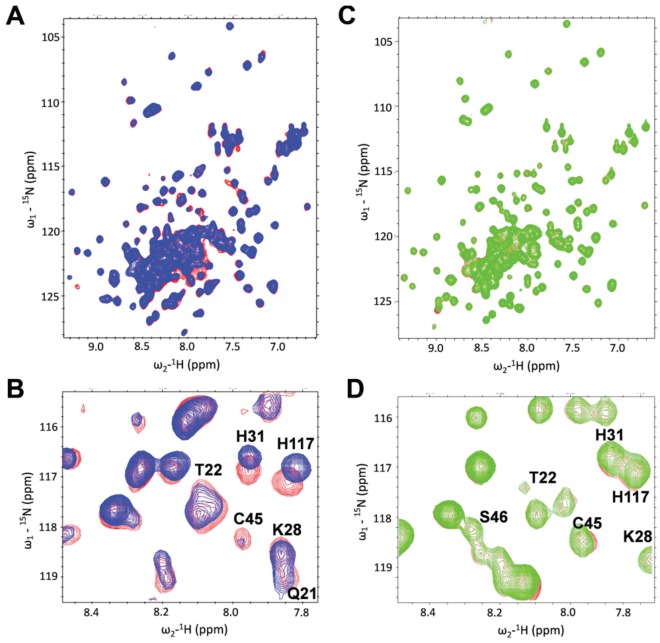

Supplementary Figure S6. Ac3AESA does not bind mutant R24A/K28A HMGB1. (A) ^{15}N-^{1}H HSQC spectra for FL WT HMGB1 (~0.1 mM) were generated in the presence (blue) or absence (red) of 3 mM ac3AESA. (B) Residues that show significant CSPs due to ac3AESA binding are labeled in expanded regions of the superimposed spectra. (C) ^{15}N-^{1}H HSQC spectra for R24A/K28A (~0.1 mM) were generated in the presence (green) or absence (red) of 3 mM ac3AESA. (D) Residues that show significant CSPs due to ac3AESA binding of WT HMGB1, but not of R24A/K28A, are labeled in the expanded regions of the superimposed spectra.

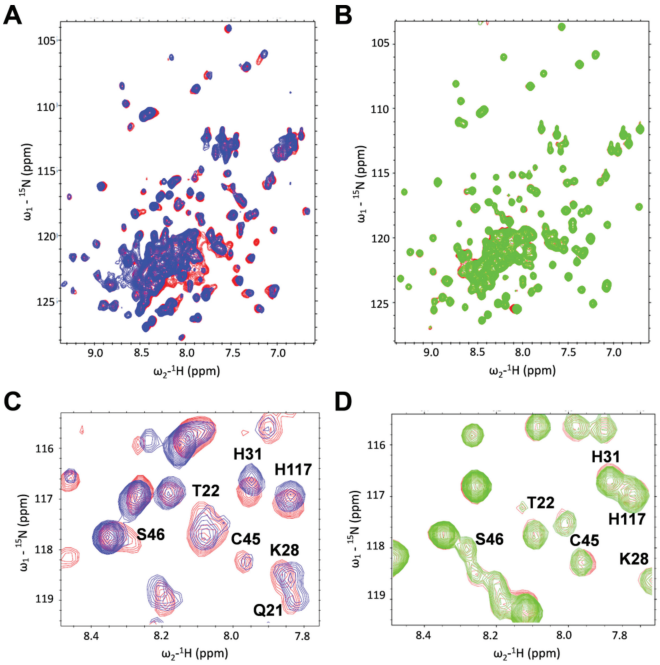

Supplementary Figure S7. Amorfrutin B1 does not bind mutant R24A/K28A HMGB1. (A) ^{15}N-^{1}H HSQC spectra for FL WT HMGB1 (~0.1 mM) were generated in the presence (blue) or absence (red) of 3 mM amorfrutin B1. (B) Residues that show significant CSPs due to amorfrutin B1 binding are labeled in expanded regions of the superimposed spectra. (C) ^{15}N-^{1}H HSQC spectra for R24A/K28A (~0.1 mM) were generated in the presence (green) or absence (red) of 3 mM amorfrutin B1. (D) Residues that show significant CSPs due to amorfrutin B1 binding of WT HMGB1, but not of R24A/K28A, are labeled in the expanded regions of the superimposed spectra.

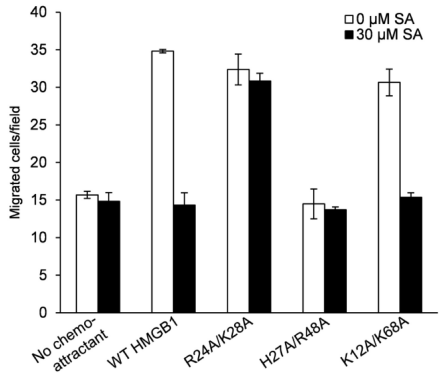

Supplementary Figure S8. Effect of SA on the chemo-attractant activity of mutants of HMGB1: R24A/K28A, H27A/R48A, and K12A/K68A. Migration of 3T3 fibroblasts was induced by 1 nM fully reduced WT and mutant HMGB1 in the absence or presence of 30 μM SA. The data represent the mean ± SD (n=3).

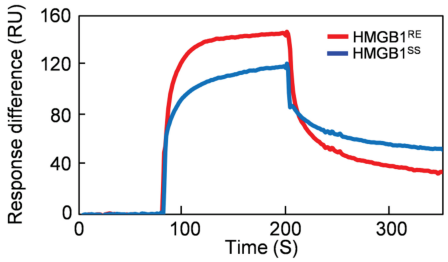

Supplementary Figure S9. Evaluation of the SA-binding activity of fully reduced HMGB1 (HMGB1^{RE}) and disulfide HMGB1 (HMGB1^{SS}) by SPR. Shown are sensorgrams of fully reduced and disulfide HMGB1 (0.5 μM) interacting with 3AESA immobilized on the SPR sensor chip. The signal from the mock-coupled surface was subtracted.

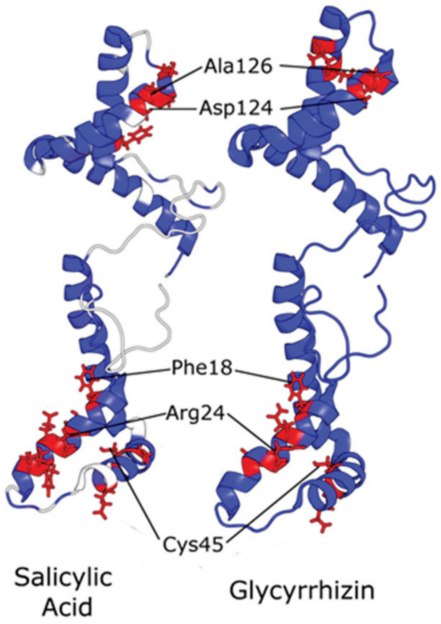

Supplementary Figure S10. SA and glycyrrhizin bind at similar sites in HMGB1. ^{15}N-^{1}H CSPs due to either SA binding (left) or glycyrrhizin binding (right) were mapped onto human HMGB1-ΔC (2YRQ, res. 6-164). All residues are blue except for those exhibiting significant CSPs, which are depicted as red stick structures. Binding site residues shared by SA and glycyrrhizin are labeled.